JISET - International Journal of Innovative Science, Engineering & Technology, Vol. 5 Issue 12, December 2018
ISSN (Online) 2348 – 7968
www.ijiset.com

Comparison of Modern methods for Stability Analysis of Electrical Power Transmission Networks: Case of the Cameroon's Southern Interconnected Grid (SIG)

Andre Cheukem[2],Y. A. Tene Deffo[1], P. Tsafack[1], and P. Ghogomu[1, 3], G. Kenne[2]

[1] University of Buea, Faculty of engineering and technology,
Buea, South-West region, Cameroon

[2] University of Dschang, UIT of Bandjoun,
Bandjoun, West region, Cameroon

[3] ENEO,
Douala, Littoral region, Cameroon

Abstract

This paper analyses the efficiency and stability frailties of power networks with emphases on transmission systems. A mathematical model of the power system elements with significant impact on the system voltage stability is simulated using Power System Analysis Toolbox (PSAT) - Matlab-based toolbox. Then, voltage stability related information from a system-wide perspectives were obtained and clear identifications of areas of potential weaknesses were made via continuation power flow (CPF) and voltage sensitivity factor (VSF) computation. As suggested solutions, a tight transmission system is developed around critical lines of the systems. It turned out that this solution, coupled with an optimal positioning of system capacitor banks around sensitive load buses has the positive effect of restoring system voltages within acceptable limits. Secondly, Flexible AC Transmission Systems (FACTS) controllers were modelled and tested to show their effect under large system perturbations via time domain simulation.

Keywords: Efficiency, Voltage Stability, CPF, VSF, and FACTS.

1. Introduction

The confluence of economic, environmental and geopolitical concerns around reducing exposure and vulnerability to disruptions in the supply of energy has move efficiency and power system stability studies to the fore. Global continuous growth in the demand for electricity has set power systems under increasing operating pressure owing to; unmatched load and generation growth, economic and environmental constraints, inexistent or inaccurate voltage, and power flow control mechanism leading to recurrent power failures as the case of Cameroon and other developing countries. In Cameroon, the constant increase in load demand for electricity let to the extension of the electric power transmission and distribution system linking generators and loads to form a large integrated grid system. This further increases the distance between the generating stations and the loads. Power systems, constrained to operate under such conditions to meet load demand, usually operates near stability limits and thus, become more vulnerable to power inefficiencies, instabilities and cascading failures.

Grid congestion of large interconnected power systems impede the efficient movement power, reducing reliability and increases system's vulnerability to various stability problems. Voltage stability is a limiting factor to modern power systems planning and operation, usually as a result of a disturbance in the system or a significant increase of power demands in an area that causes deficiencies of reactive power supplies in an area. This paper is subdivided into sections as follows: section 2, describes transmission system characteristics, losses and limits. Then, electrical power system stability is introduced and problems of voltage stability and voltage instability in electric power systems are discussed. Section 3 deals with the models' simulation and the results from the simulations of the system cases and the last section provides conclusions and suggestions from the results of the simulated models.

2. Efficiency and Stability of Power Transmission System Overview

Efficiency is the term applied to how energy is produced and distributed [1]. A key component in measuring the efficiency and financial sustainability of the power sector is electricity loss. It reflects the degree of productivity of transmission and distribution systems, representing the difference between the amount of electricity that enters the network and the amount that is delivered to end-users [2].

1.1 Transmission System Characteristics

The ability of interconnected transmission network to transfer quality electrical power reliably and economically may be limited by physical, environmental and electrical characteristics of the systems [3]. Transfer capability computations are mainly a function of three limits: thermal limit overload, voltage limits and transient stability limits. In general, transient stability limits are more important than thermal limits for long transmission lines, while thermal limits are more important for shorter lines. Since stability is a system property rather than a material property, stability limits change depending on the length of a line and other system conditions. Further, the power transfer on medium-length lines is usually constrained by voltage stability, while the longest lines are limited by transient stability. Finally, transmission lines loadability decreases as length increases. Fig. 1 illustrates the typical limiting factors on the power transfer of short, medium, and long lines.

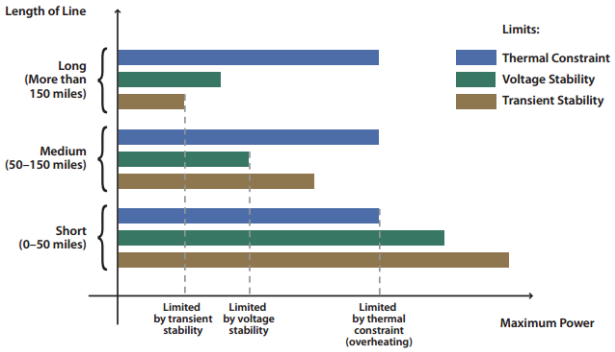

Fig. 1 Three Primary Constraints of Transmission Lines *Invalid source specified.*.

On the other hand, stability in power systems is an operating condition characterised by an equilibrium state between the electric power generation and consumption by the load. By occurrence of a system change or a disturbance, the stability depends on the initial operating condition and the nature of the disturbance [4]. Instability results when a system change or the disturbance leads to an imbalance between the generation and the load.

2.1 Power System Stability

Electric Power System Stability is defined as the capability of a system to maintain an operating equilibrium point after being subjected to a disturbance for given initial operating conditions [5]. Fig. 2 shows the overall picture of the power system stability problem, identifying its categories and sub-categories.

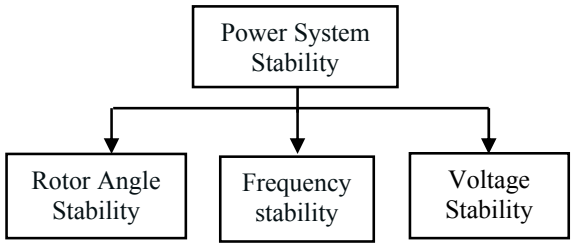

Fig. 2 Classification power system stability **[5]**.

Voltage stability refers to the ability of a power system to maintain steady voltages at all buses in the system after being subjected to a disturbance from a given initial operating condition [5]. Disturbances are typically categorized as small disturbances (daily load variations) or large disturbances (component outage) as depicted by Fig. 3.

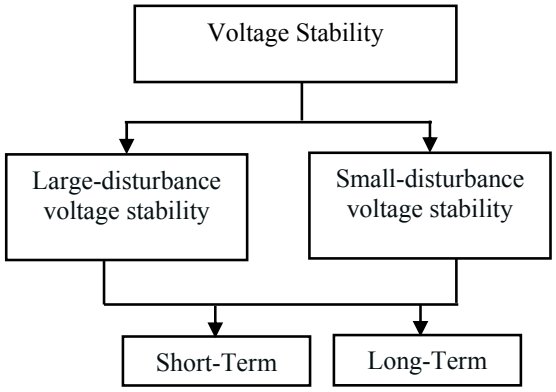

Fig. 3 Classification voltage stability **[5]**

The time span of this disturbance, ranging in time from a fraction of seconds to tens of minutes and causing a potential voltage instability problem, can be classified into short-term and long-term voltage stability [6]. Short-term voltage stability involves dynamics of fast acting load components such as induction motors, electronically controlled loads, and HVDC converters and actual voltage collapse comes very soon after the disturbance, just a few seconds or less. On the other hand, long-term voltage stability involves slower acting equipment such as tap-

changing transformers, thermostatically controlled loads, and generator current limiters. It develops from a gradual lack of reactive power at a node or in a part of the system [7] and may extend to several or many minutes.

3. Methodology

There are two main approaches of voltage stability analysis: static and dynamic.
Static or steady-state methods permits the evaluation of the system stability with help of load flow equations using a snapshot of the system at a point in the time domain trajectory and give an indication of the system stability at this specific operating point [4].
The dynamic analysis implies the use of a model characterized by non-linear differential and algebraic equations which include generators dynamics or tap changing transformers.

3.1 Computational Power Flow (CPF)

CPF procedure [8], [9] is based in a reformulation of the equations of the load flow problem by which the power flow solutions can be obtained near or at the voltage collapse point. The purpose of continuous load flows is to find a set of load flow solutions in a scenario where the load is continuously changing, starting from a base case until the critical point. It consists in a predictor step realized by the computation of the tangent vector and a corrector step that can be obtained either by means of a local parametrization or a perpendicular intersection.
Using constant power load, the general form of Newton-Raphson power flow equations are reformulated as:

$$P_{Gi} - P_{Di} - P_i = 0 \quad (1)$$

$$Q_{Gi} - Q_{Di} - Q_i = 0 \quad (2)$$

The subscript Qi, Di and i denote generation, load and injection demand respectively on the related bus.
In order to simulate a load change, the power flow equations are parameterized with a factor λ, which represents the variation of load demand P_{Di} and Q_{Di}

$$P_{Di} = (P_{Di0} + \lambda K_{Di} P_{\Delta base}) \quad (3)$$

$$Q_{Di} = (Q_{Di0} + \lambda K_{Di} Q_{\Delta base}) \quad (4)$$

Where, P_{Di0}, Q_{Di0} are the original active and reactive load demand on i^{th} bus. $P_{\Delta base}, Q_{\Delta base}$ are the given quantities of powers chosen to scale λ appropriately and K_{Di} multiplier to designate the rate of load change at bus i as λ changes.
Then the active power generation term can be modified to:

$$P_{Gi} = P_{Gi0}(1 + \lambda K_{Gi}) \quad (5)$$

The next step is to apply a continuation algorithm to the system of reformulated power flow equations and the problem can be expressed as:

$$F(\theta, V, \lambda) = 0 \quad 0 \le \lambda \le 1 \quad (6)$$

Predictor Step:

This step is to find a next point (θ', V', λ') starting from an initial point (θ, V, λ). In the predictor step, a linear to approximation is usual to estimate the next solution for a change in one of the state variable [10]. Thus, the process is to calculate the tangent vector here expressed in factorized form as a matrix of partial derivatives multiplied by a vector of differentials:

$$[F_\theta \; F_V \; F_\lambda] \begin{bmatrix} d\theta \\ dV \\ d\lambda \end{bmatrix} = 0 \quad (7)$$

The former is the conventional load flow Jacobian augmented by one column F_λ, while the latter is the tangent vector being sought.

Corrector Step:

The predictor step leads to the next point (θ', V', λ') which is generally not on the PV curve. Since a good predictor gives an approximation in a neighbourhood of the next solution [11], the Newton method is chosen in CPF as the corrector. Local parameterization scheme [12] was applied in this paper. In the corrector step, the original set of equations is augmented by one equation that specifies the state variable selected as the continuation parameter. Thus new set of equations is:

$$\begin{bmatrix} F(\theta, V, \lambda) \\ x_k - n \end{bmatrix} = F_\theta \quad (8)$$

In Eq. (8), x_k is the additional equation that guarantees a non-singular Jacobean at the bifurcation point. The predictor and corrector schemes of CPF are illustrated in Fig. 4.

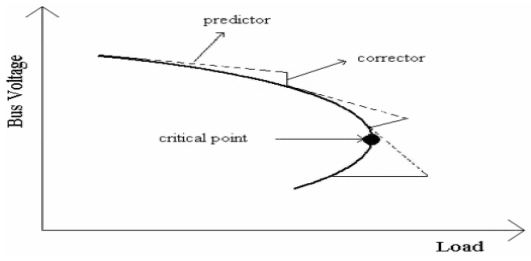

Fig. 4 The predictor – corrector scheme [12]

3.2 Voltage Collapse Proximity Indicator (VCPI)

[13] proposed line stability indices based on the concept of maximum power transferred through a line. The stability indices of each transmission line of the system are defined as:

$$VCPI(power) = \frac{P_R}{P_{R(\max)}} \quad (9)$$

$$VCPI(losses) = \frac{P_{loss}}{P_{loss(\max)}} \quad (10)$$

$P_{R(\max)}$ is the maximum real power that can be transferred and $P_{loss(\max)}$ is the maximum possible real power loss each expressed as:

$$P_{R(\max)} = \frac{E^2 \cos\phi}{4Z_L \cos^2(\frac{\theta-\phi}{2})} \quad (11)$$

$$P_{loss(\max)} = \frac{E^2 \cos\theta}{4Z_L \cos^2(\frac{\theta-\phi}{2})} \quad (12)$$

From Eq. 9 to Eq.12, the overall line stability indices of the power transmission system can be expressed as:

$$VCPI(total\_power) = \frac{\sum_{i=1}^{n} P_{R\_i}}{\sum_{i=1}^{n} P_{R(\max)\_i}} \quad (13)$$

$$VCPI(total\_losses) = \frac{\sum_{i=1}^{n} P_{loss\_i}}{\sum_{i=1}^{n} P_{loss(\max)\_i}} \quad (14)$$

Where *n* is the number of lines in the power system. The fundamental cause of voltage collapse is considered due to excessive power transfer through the line or excessive absorption of power by the line itself as a result of line inefficiency [13].

As the maximum power transfer theory restricts the amount of power that can be transferred or absorbed, the proposed indicators should predict the voltage collapse point and transmission line efficiency precisely.

3.3 Large-disturbance Voltage Stability Index

Fig. 5 illustrates the definition of transient voltage dip [14]. The transient voltage dip (TVD) is defined as the percentage of maximum deviation of short-term voltage after voltage recovery following fault clearing over initial voltage of each individual bus.

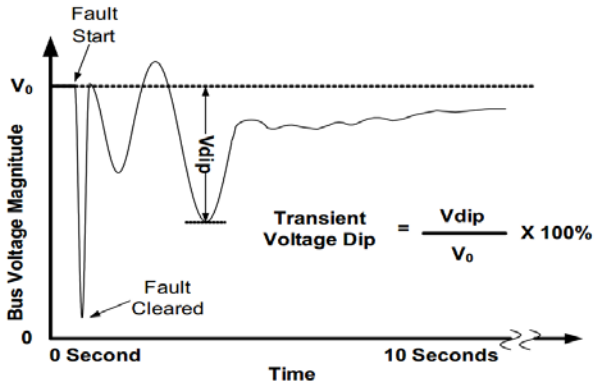

When the transient voltage dip is small and within the voltage stability criteria (25%), the case is marked as healthy or voltage stable. When the largest transient voltage dip is over the voltage stability criteria (25%), the case is marked as voltage unstable [15].

4. System Modelling

Many power system phenomena are initiated by the aggregated effect of changing loads. Hence, the model should have the ability to partially account for the response of interconnected generators to fluctuating demands. The following description includes only a subset of the relevant characteristics for power system modelling. These are power system elements that have significant impacts on voltage stability and efficiency and, directly related to the case under studies.

4.1 System model

The overall system equations may be expressed as a sum of differential and algebraic equations:

$$\dot{x} = f(x, V) \quad (15)$$

$$I(x, V) = Y_N V \quad (16)$$

With a set of known initial conditions (x_0, V_0), where x is the system state vector, V the bus voltage vector, I the current injection vector and Y the network admittance matrix.

4.2 Generator Equivalent model

For an efficient representation of the generator dynamics, the synchronous machine model, automatic voltage

regulator (AVR), as well as the over excitation limiter (OXL) are to be accounted.

Generator model:

In this paper, all the case system generators have identical dynamic characteristics using the fourth-order generator model sufficient to represent synchronous machines in transient stability studies as reported by [16] and applied for voltage stability analysis in [17].
The rotor characteristics are represented by the field windings and a damper winding in the d-axis and two damper windings in the q-axis. The mutual inductances between the stator and the rotor windings are assume to be equal. The equations of the generator model are:

$$\dot{\delta} = \Omega_Q(\omega - 1)$$
$$\dot{\omega} = (p_m - p_e - D(\omega - 1))/M$$
$$\dot{e}_q = (-f_s(e'_q) - (x_d - x'_d)i_d + v^*_f)/T'_{d0}$$
$$\dot{e}'_d = (-e'_d + (x_q - x'_q)i_q)/T'_{q0} \qquad (17)$$

Where $\delta = \theta(t) - \Omega_b t$

Automatic Voltage Regulator (AVR):

AVR defines the primary voltage regulation of synchronous machines. As shown in Fig. 6, the IEEE standard AVR (Mode I) is use to model generator voltage regulation with the amplifier block subjected to an anti-windup limit.

Fig. 6. IEEE standard AVR (Model I) **[17]**

Over Excitation Limiter:

Over excitation limiters (OXL) provides an additional signal to the reference voltage of automatic voltage regulator (AVR). The OXL is modelled as a pure integrator, with anti-windup hard limits (Fig. 7).

$$\dot{v}_{oxl} = (i_f - I_{fLIM})/T_0, \qquad \text{If } i_f > I_{fLIM}$$
$$\dot{v}_{oxl} = 0, \qquad \text{If } i_f \le I_{fLIM} \quad (18)$$

4.3 Transmission system model

Fig. 7. depicts the circuit used for defining the transmission line lumped model. The expressions of the active power transfer P_{km} and reactive power transfer Q_{km} of a transmission line can be determined as:

$$P_{km} = V_k^2(g_{km} + g_{k0}) - V_k V_m(g_{km}\cos(\theta_{km}) + b_{km}\sin(\theta_{km}))$$
$$Q_{km} = -V_k^2(b_{km} + b_{k0}) - V_k V_m(g_{km}\sin(\theta_{km}) - b_{km}\cos(\theta_{km})) \qquad (19)$$

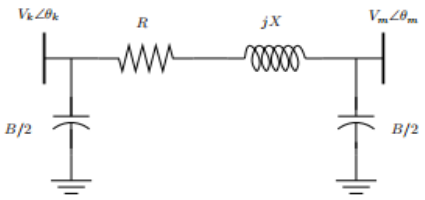

Fig. 7. Transmission line π circuit **[18]**

Two-winding transformers are modelled as series reactances without iron losses and their equations are included in Eq. (21). The primary and secondary voltage ratio k_T allows distinguishing between transmission lines and transformers, zero for transmission lines.

ULTC model:

The tap ratio is subjected to an anti-windup limiter. If the tap ratio step $\Delta m > 0$, a discrete model is used, as follows:

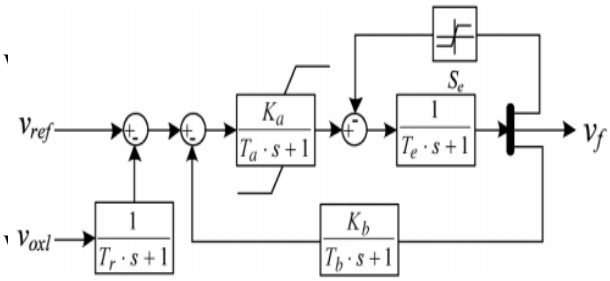

v_{ref} the reference signal and Δu the error tolerance.

5. Case study, Results, and Discussions

5.1 Presentation of the SIG system

The Southern Interconnected Grid (SIG) is the largest out of three independent transport and distribution networks that make up the Cameroon power network. It is a 32-bus, 225-90 kV transmission network connecting the major

hydropower stations of Edea and Song-Loulou, the natural gas power plant of Kribi, and six main thermal power plants to load centers distributed over six regions of the country.

The actual SIG system incorporates two additional 90kV buses at Logbaba (bus 11) and Oyomabang (bus29), and control switches. The utility operator uses the control switches to operate these buses based on the system loading conditions at these respective locations. Hence, two operating modes are possible; disconnected mode (DM) and connected mode (CM) for light and heavy system loading during full load and peak load hours respectively. Schematics of the SIG system incorporating these operating modes are available under appendix as well as the system load data for each operating mode. The present system model and simulation also accounts for low voltage load and generator buses and the effects of ULTC on these later, extending the 32 bus SIG system to a 77 bus SIG system.

Mode of Operation	Bus N°	Equipment	Capacity
DM	11	generators 1,2 & 3 - G7	37.4 MW
	16	Generator - G11	10 MW
	32	capacitor bank	25 MVAR
	2	capacitor bank	25 MVAR
	11	capacitor bank	25 MVAR
	13	L11 - 90kV Oyomabng-BRGM N°1	94 MVA
	21	loads	23.2 MVA
	2	loads	
CM	11	generators 1 - G7	5.4 MW

5.2 Comparison between the modelled network and the actual network

In the light of system prerequisites to stability analysis, the proposed models (DM and CM) were simulated to effectively replicate actual system operating conditions for disconnected and connected modes. The bus voltage profiles for connected mode (CM) and disconnected mode (DM) were respectively compared to the actual utility data of January 12, 2015 during full hours (11:34 - DM) and January 18, 2017 during peak hours (20:30 - CM). Fig. 8. depicts the comparison results for DM and CM load conditions.

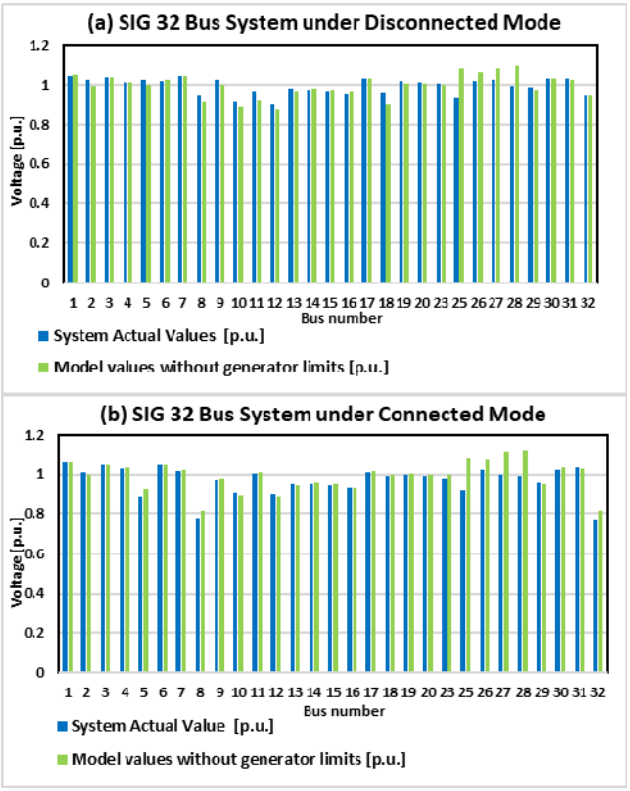

Fig. 8. Comparative analysis between actual and simulated bus voltages

Likewise, Table 1. compares the model and actual systems results. The actual system contingencies for CM and DM considered during analysis are presented in Table 2.

Table 1. Comparison between the model and actual network results

Table 2. Actual network contingencies under CM and DM.

Upon simulations, the calculated simulation errors were respectively 43% and 30% for the system under DM and CM. Among the factors contributing to this significant error margin are; the arbitrary NLTC fixed tap ratio at generator buses and ULTC reference voltage settings (set at 0.95 p.u) at load buses, and the lack of precise and up-

Global results comparison	*DM*		*CM*	
	Actual	*Model*	*Actual*	*Model*
Active power generated [MW]	631.4	584.6	917.5	842.2
Reactive power generated [MVAR]	198.4	125.2	359.9	253.1
Load Active power [MW]	572.7	574.9	802.8	812.1
Load Reactive power [MVAR]	223	222.1	254.6	255.9
Capacitor bank [MVAR]	-108	-115.7	-153.2	-175

to-date system data. It is therefore with 57% and 70% simulation accuracy respectively for DM and CM that the SIG models were adopted and further used in this research to study the stability of the SIG system.

5.3 Results of the modelled SIG network

Long-term voltage stability analysis:

The selected tolerance iteration values used for the power flow simulation are 0.001 and 0.01. This is used to determine how accurate a solution will be. Thus, using a high tolerance value for a simulation increases the accuracy of the solution whereas when a low tolerance value is used, it reduces the accuracy of the solution and number of iterations [19]. A maximum number of iterations of 20 was considered as the number of iteration increases as the number of buses in the system increases. Newton-Raphson method was chosen as it has the least number of iteration to converge and suitable for large size system, what makes it the utmost tool for power flow analysis. Two simulation conditions were considered each represented by superscripts [1] and [2], respectively indicating that with generator limits and without.
Fig. 9. Depicts the bus voltages after power flow and continuation power flow analysis for DM and CM respectively.

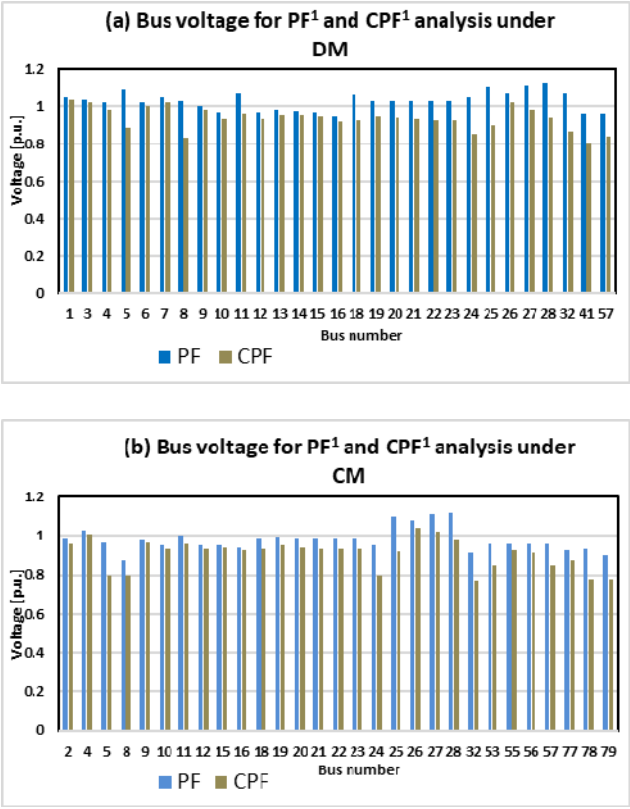

Fig. 9. Power Flow (PF) and Continuation Power Flow (CPF) analysis of the bus voltages

Short-term voltage stability analysis:

The short-term voltage stability problem of the system is thoroughly investigated in time domain for two different contingencies (line outage and 3-phase fault). The results obtained for the above contingencies are briefly described as follows. The contingency event is: simulation starts with no fault, then, a three-phase to ground fault occurs at a bus. The fault is later cleared after 0.1 seconds by tripping the line connected to the bus. The total simulation time period was ten seconds. The results of transient voltage dip (TVD) analysis of each contingency location are compared for both system models. These are shown in Fig. 10. (a)-(g). Represented in the figure are buses with significant transient voltage dips for the N-1 contingency under analysis.

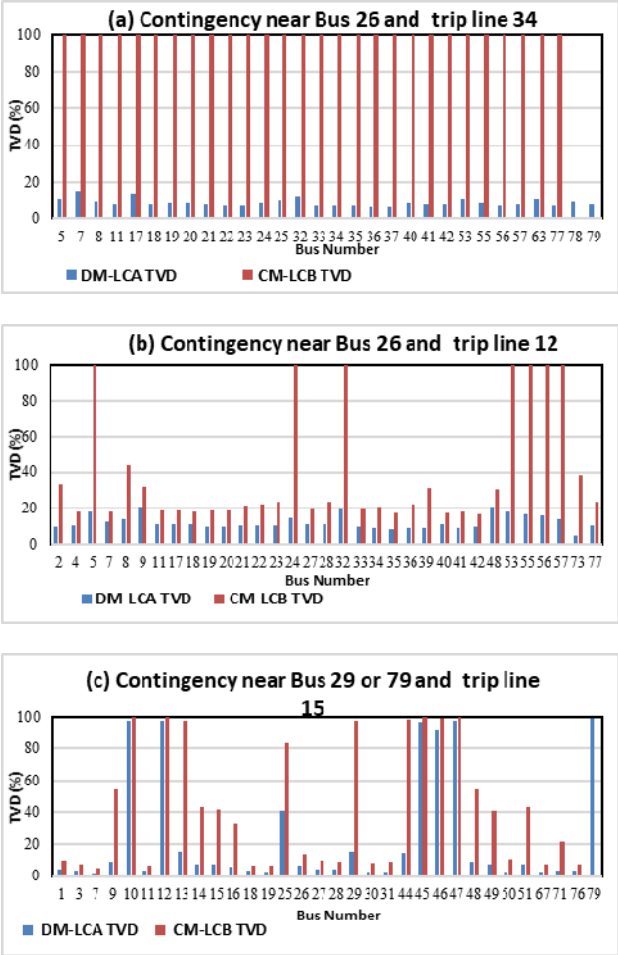

Fig. 10. TVD of the SIG system for contingency near Bus 26 and Bus 29

The simulation results show that different contingency locations affect significantly the post-contingency voltage behaviour. For the same initial operating point, the voltages for DM remain stable for any fault except that at bus 29 or 79 followed by the tripping of line 15 where some transient voltage dips exceed the voltage dip criteria. A voltage collapse is inevitable when a fault at bus 26 leads to tripping of line 36. In this research, scenarios (a) and (c) of Fig. 10. are of main interest.

So far, one can point out the following system deficiencies in the SIG: insufficient or distance transmission of reactive power to load centres, high transmission line loading, unsuitable locations of capacitor banks, low generator terminal voltages, and low transmission system efficiency.

To the above SIG problems, two solution proposals were made.

5.4 Proposed modified SIG Model

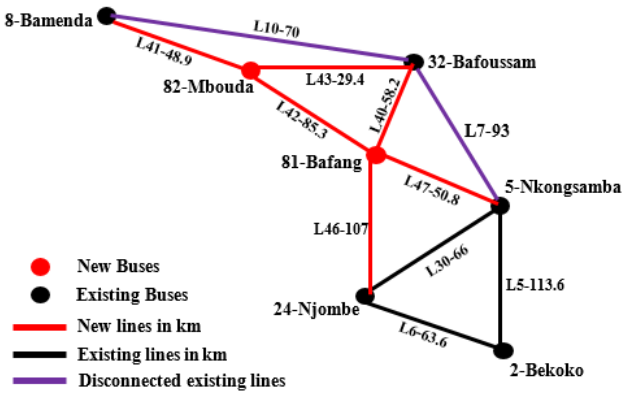

(a)- Modified transmission system against line 7 outage

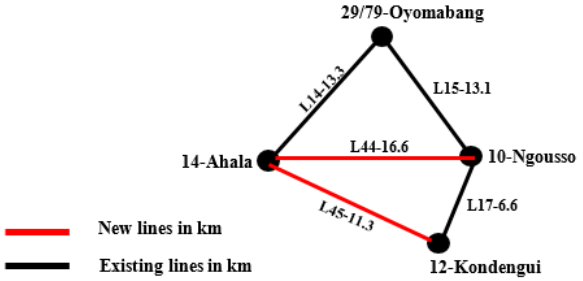

(b)- Modified transmission system against line 15 outage

Fig. 11. Proposed modified SIG system: modified transmission system

Transmission System Expansion:
Transmission line reinforcement especially on lines 7 and 15 is essential to avoid system collapse for any contingency on these lines. Fig. 11. depicts the proposed modified system with its additional transmission lines needed to solve the problems at hand.
Transmission System Compensation (FACTS Devices):
A 100MVAR SVC is added to show the effect of this controllers on the system. The added controllers' model was placed on bus 81-Bafang, based on the transient voltage dip and voltage sensitivity analyses.
Another proposed solution to solve current system failures is through optimal allocation of installed compensating devices (capacitor banks) in the system. A compensation restructuring scheme was designed for each SIG system configuration. These are shown in Table 3.

Table 3. Optimal allocation of capacitor banks on the Modified SIG syste

5.5 Results of the proposed modified SIG Model

Long-term voltage stability analysis:
A comparative analysis of the system voltages for the current and modified SIG model was made after PF and CPF analyses. The figures below depict these results.

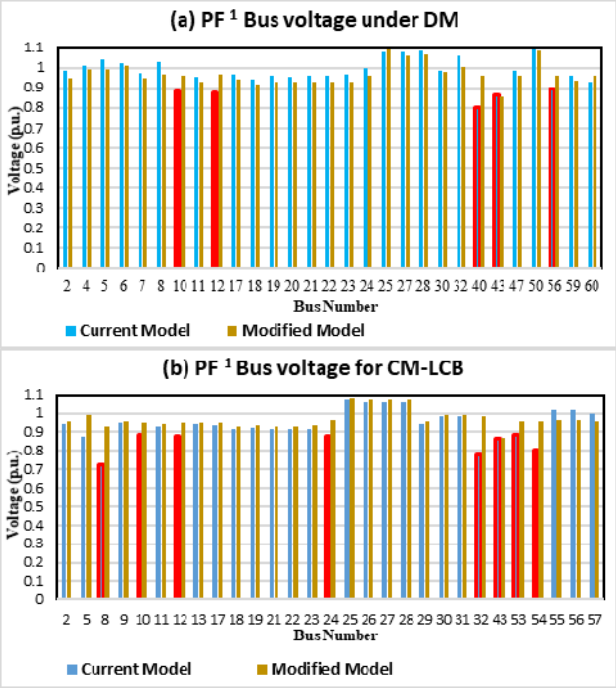

Fig. 12. PF[1] bus voltage comparison between current and modified SIG

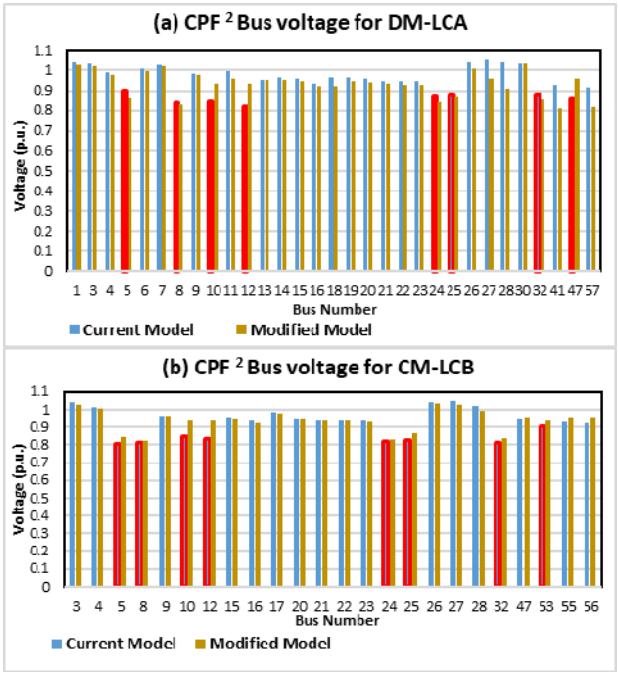

Fig. 13. CPF[2] bus voltage comparison between current and modified SIG

Fig. 14 compares line stability indices of the current and modified SIG models for both system configurations, all based on CPF[2] analysis.

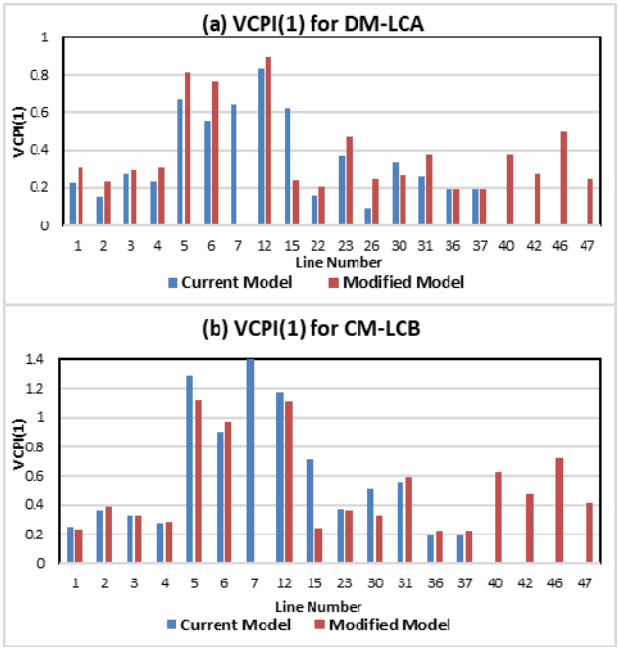

Fig. 14. VCPI comparison between current and modified SIG

Fig. 15. and Fig. 16. respectively compares the MLP and the efficiency of the current and modified SIG for both system configurations, all based on CPF[2] analysis.

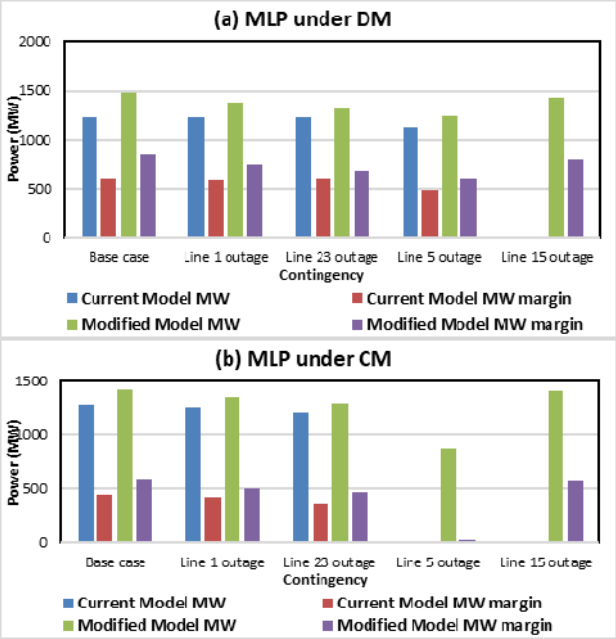

Fig. 15. MLP comparison between current and modified SIG

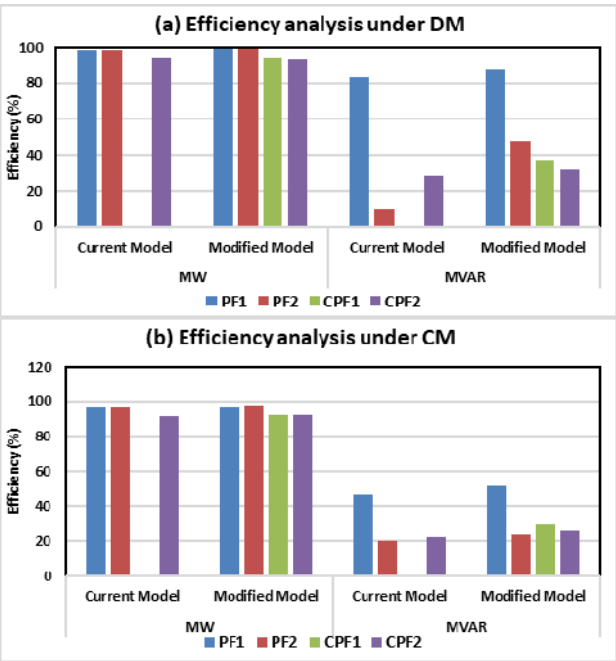

Fig. 16. Efficiency comparison between current and modified SIG

Short-term voltage stability analysis:
Three system models were considered; the current model, the modified model and the modified model with SVC. The results obtained are described in Fig. 17.

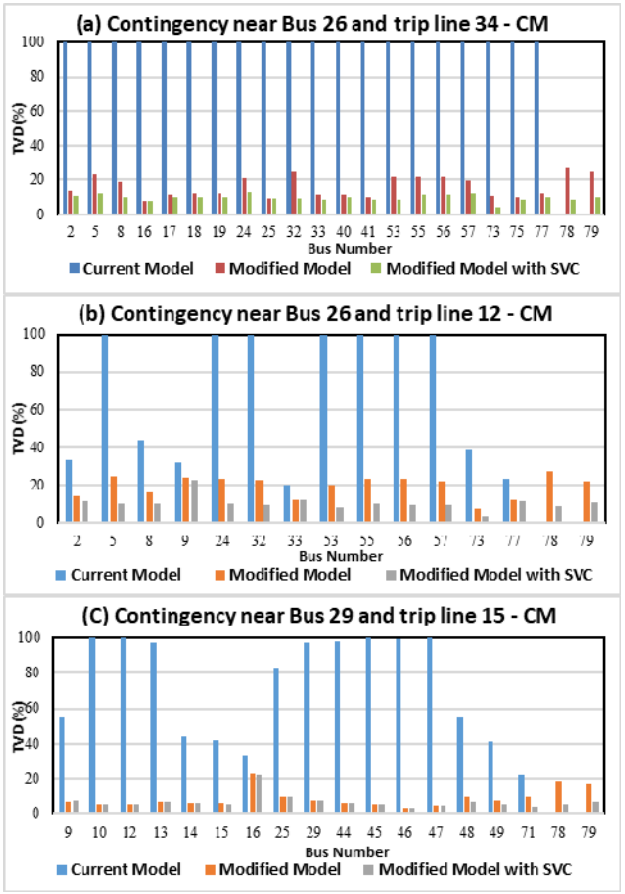

Fig. 17. TVD of the SIG for different models under different contingencies

It can be observed from Figure 4-10 that all system bus voltages are within acceptable limits for PF[1]. The per unit bus voltages at Bus 10 and 12 were respectively restored from 0.888 and 0.878 to 0.948 and 0.952 thanks to the tight transmission system built around line 15 and the 12.5 MVAR capacitor bank at bus 12. This does not only improve the system stability, but further improve system efficiency as it helps redistribute power flow between bus 10, 12, 14 and 29 (see Fig. 12. and Fig. 13.).
Likewise, the per unit bus voltages at Bus 5, 8 and 32 were respectively restored from 0.873, 0.723 and 0.776 to 0.9924, 0.931 and 0.9807 as a result of the additional transmission lines installed around lines 7 and 10. It should be noted that the new transmission lines were designed based on the actual lines 7 and 10 characteristics. Hence, these later can be reused in the modified SIG models. In both cases, the ability of the SIG system to

withstand any line contingency without system collapse is an indelible outcome of the proposed solution. One that the current system models cannot provide. However, further attention will be required at bus 43 and on line 12 as these later become a bottleneck to future system stability and efficiency.
Fig. 15. clearly shows that the modified models do not only leads to a more stable grid, but also contribute in extending the system maximum loading points (MLP). The system efficiency not left aside keeps pace with the MLP. From Fig. 16., noticeable increase in the system MVAR efficiency can be observed. Among the contributing factors to this increase is the limited and optimal positioning of capacitor banks near load buses in the system.

At this junction, to further illustrate the positive impact of the modified model, this later was simulated following the actual system contingencies described in Table 2. The results were compared to that of the current SIG models and the actual SIG bus voltages. Fig. 18. depicts these analyses. It turns out the modified SIG models significantly increases the system stability by restoring the bus voltages at Bus 5-Nkongsamba, Bus 8-Bamenda, Bus 10-Ngousso, Bus 12-Kongengui and Bus 32-Bafoussam within acceptable limits.

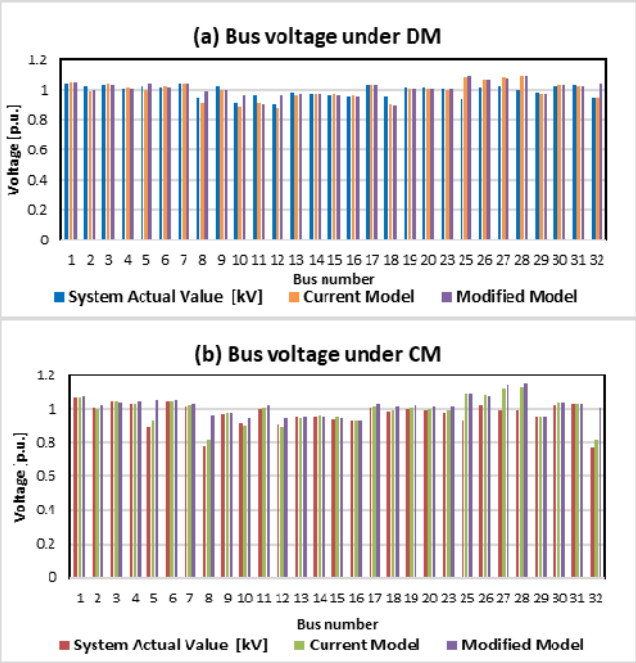

Fig. 18. Bus voltage comparison between actual, current and modified SIG

One should however note that though, SVC will respectively boost and reduce the voltage profiles and transient voltage dips of the system. Their implementation alone cannot prevent system collapse for neither line 7 nor Line 15. Likewise, a tight transmission system around the critical lines may be sufficient to prevent system collapse when these later are tripped and by so doing improve system voltage stability. Yet, it is not enough (alone) to restore every system bus voltage within acceptable limits. Hence, for best system performance, both proposed solutions should be considered. Reducing line losses makes it less likely that system loads will exceed system capacity, thus enhancing reliability by avoiding brownouts and blackouts that can occur under such circumstances.

6. Conclusions

This paper investigated the stability of the electrical power transmission system network. The Cameroon's SIG as case studied and its performance observed from the bus voltage profiles. The bus voltage is decreasing as the load power demand increases. This was mainly due to due to lack of local reactive power support in the system. Performance of the power system with and without FACTS devices installed can be tested by modelling a power system network in PSAT.

References

[1] Energy Effiiency in the Power Grid, Norwalk: ABB Inc., 2007.

[2] R. Jiménez, T. Serebrisky and J. Mercado, Power lost: Sizing Electricity Losses in Transmission and Distribution Systems in Latin America and the Caribbean, New York: IDB Monograph ; 241, 2014.

[3] "Available Transfer Capability Definitions and Determination," NERC, New york, 1996.

[4] Y. Tchokonte, Real-time idenification and monitoring of the voltage stability margin in electric power transmission systems using synchronous phasor measurements, Kassel: Kassel University press GmbH, 2009.

[5] Hatziargyriou and e. al, "Definition and Classification of Power System Stability IEEE/CIGRE Joint Task Force on Stability Terms and Definitions," *IEEE Transactions on Power Systems,* September 2004.

[6] P. Kundur, "Definition and classification of power system stability.," *IEEE transactions on power systems,* vol. 19, no. 2, pp. 1387-1392, 2004.

[7] G. Andersson, Modelling and analysis of electrical power systems, Zurich, September 2008.

[8] D. Satish, "Voltage Stability Analysis of Power System using Continuation Power Flow Method," *IJTRE,* vol. 1, no. 9, pp. 763-768, May-2014.

[9] N. Fnaiech, A. Jendoubi and F. Bacha, "Voltage Stability Analysis In Power System Using Continuation Method and PSAT Software," in *6th International Renewable Energy Congrss (IREC)*, 2015.

[10] P. Kundur, Power System Stability and control, New York: McGraw-Hill, 1994.

[11] H. D. Chiang and e. al, "CPFLOW: A Practical Tool for Tracing Power System Steady-State Stationary Behavior Due to Load and Generation Variation," *IEEE Trans. Power Systems,* vol. 10, no. 2, pp. 623-634, May 1995.

[12] Ajjarapu and e. al, "The Continuation Power Flow: a tool for Steady State Voltage Stability Analysis," *IEEE Transactions on Power Systems,* vol. 7, no. 1, pp. 416-423, February 1992.

[13] M. Moghavvemi, "Real-time contingency evaluation and ranking technique," *IEE Proc.-Gener. Transm. Distrib.,* vol. 145, no. 5, pp. 517-524, September 1998.

[14] NERC/WECC, *Planning Standards,* April, 2003.

[15] M. Nizam, "A Static and Dynamic Technique Contingency Ranking Analysis in Voltage Stability Assessment," 2008.

[16] T. Weckesser and e. al, "Impact of Model Detail of Synchronous Machines on Real-time Transient Stability Assessment," in *2013 IREP Symposium-Bulk Power System Dynamics and Control –IX (IREP)*, Rethymnon, Greece, August 25-30, 2013.

[17] Y. Wang and e. al, "Incorporating Generator Equivalent Model Into Voltage Stability Analysis," *IEEE Transaction on Power Systems,* vol. 28, no. 4, pp. 4857-4866, Nov 2 0 1 3.

[18] F. Milano, "Matlab-Based Power System Analysis Toolbox Version 2.2.0," Feb. 2008.

[19] O. A. and e. al, "Analysis of the Load Flow Problem in Power System Planning Studies," *Energy and Power Engineering,,* vol. 7, pp. 509-523, 2015.

[20] EDF, "Rapport d' Analyse du Réseau existant pour 2015 et 2020 et d' amélioration de la Stabilité du RIS," ENEO, Douala, Cameroun, Mars 2015.

Y. A. Tene Deffo Received the B.Eng and M.Eng degrees in power systems engineering in 2015 and 2017 respectively from the University of Buea. He is currently pursuing a Ph.D. degree in material characterisation and non-destructive testing (NDT), thesis under co-supervision between University of Buea - Cameroon and INSA-Lyon - France. His interests include local magnetic characterization, NDT, and power system stability and control. At present he is an assistance lecturer at the Faculty of Engineering and Technology, University of Buea - Cameroon.

Andre Cheukem Biographies should be limited to one paragraph consisting of the following: sequentially ordered list of degrees, including years achieved; sequentially ordered places of employ concluding with current employment; association with any official journals or conferences; major professional and/or academic achievements, i.e., best paper awards, research grants, etc.; any publication information (number of papers and titles of books published); current research interests; association with any professional associations. Do not specify email address here.

Pierre Tsafack biography appears here. Degrees achieved followed by current employment are listed, plus any major academic achievements. Do not specify email address here.

Patrick Ghogomu biography appears here. Degrees achieved followed by current employment are listed, plus any major academic achievements. Do not specify email address here.

7. Appendices

A 1. Load Distribution Data for the SIG

Bus N°	CM		DM	
	P (MW)	Q (MVAR)	P (MW)	Q (MVAR)
52	8.44	3.43	5.11	2.9
51	29.06	6.22	13.39	7.69
49	8.15	3.06	4.13	2.63
50	8	3.05	10.24	3.99
47	31.64	5.19	21.36	13.82
45	59.93	0	39.4	0
46	19.68	0	8.84	0
44	66.27	14.18	41.68	14.71
48	8.58	1.85	3.28	0.72
43	179.36	82.596	179.36	82.596
42	28.58	5.74	10.89	3.55
40	60.64	27.81	61	28.4
35	52.07	14.13	16.62	2.36
41	53.1	27.27	57.73	33.15
33	29.23	14.27	18.64	5.53
36	34.93	8.43	28.18	8.8
23	7.62	4.4	5.33	1.93
34	7.25	3.55	7.25	3.55
38	9.3	5.49	10.98	6.56
37	26.62	10.57	15.39	8.64
32	12.42	8.74	13.57	9.55
55	3.68	1.82	1.96	1.36
56	18.03	2.86	10.88	1.14
57	18	4.8	13.92	7.11
53	43.35	4.91	21.22	0.64
54	14.41	6.23	12.02	2.15

A 2. Line Data of the SIG [20]

Line N°	From	To	R [p.u.]	X [p.u.]	B [p.u.]
L1	26	27	0.0109	0.0515	0.0871
L2	9	29	0.0834	0.3299	0.0202
L3	31	11	0.2142	0.3014	0.0159
L4	4	2	0.0808	0.2044	0.0122
L5	2	5	0.1156	0.5451	0.0269
L6	2	24	0.1066	0.2699	0.0161
L7	32	5	0.1559	0.3946	0.0236

L8	31	7	0.0581	0.2301	0.0141
L9	6	4	0.012	0.0473	0.0029
L10	32	8	0.1174	0.297	0.0177
L11	29	13	0.005	0.0143	0.0008
L12	26	25	0.0292	0.1377	0.233
L13	29	13	0.0034	0.0133	0.0008
L14	29	14	0.0109	0.043	0.0026
L15	29	10	0.0261	0.1032	0.0063
L16	14	15	0.0114	0.045	0.0028
L17	12	10	0.0139	0.0551	0.0034
L18	16	14	0.0891	0.3528	0.0216
L19	15	16	0.055	0.2176	0.0013
L20	17	11	0.0087	0.0344	0.0021
L21	7	17	0.0046	0.0181	0.0011
L22	11	18	0.0082	0.0323	0.002
L23	1	27	0.0162	0.0762	0.129
L24	11	19	0.0041	0.0179	0.0011
L25	11	19	0.0057	0.0134	0.0009
L26	28	27	0.003	0.0069	0.0004
L27	19	19	0.0103	0.024	0.0015
L28	23	2	0.0194	0.0766	0.0047
L29	21	22	0.004	0.0092	0.0006
L30	24	5	0.0838	0.2122	0.0127
L31	9	30	0.1487	0.3764	0.0225
L32	20	19	0.0058	0.0228	0.0014
L33	22	23	0.0052	0.0334	0.0597
L34	1	26	0.0101	0.0474	0.0802
L35	1	26	0.0102	0.0482	0.0816
L36	3	26	0.0094	0.0631	0.1989
L37	3	26	0.0094	0.0626	0.1972
L38	31	30	0.0047	0.0119	0.0007
L39	31	30	0.0026	0.0103	0.0006

New Transmission Lines Characteristics

Line N°	From	To	R [p.u.]	X [p.u.]	B [p.u.]
L40	81	32	0.0974	0.2465	0.0147
L41	8	82	0.082	0.2075	0.0124
L42	81	82	0.143	0.362	0.0216
L43	32	82	0.0493	0.1248	0.0075
L44	14	10	0.018	0.0714	0.0044
L45	14	12	0.0123	0.0486	0.003
L46	24	81	0.169	0.4277	0.0255
L47	5	81	0.0852	0.2156	0.0129

A 3. Nomenclature of the 32-Bus SIG system

Designation	Bus No	V_{base} (kV)
SONG-LOULOU	1	225
BEKOKO-2	2	93
KRIBI	3	225
LIMBE	4	93
NKONGSAMBA	5	93
SONARA	6	93
DIBAMBA	7	93
BAMENDA	8	93
NJOCK-KONG	9	93
NGOUSSO	10	93
LOGBABA-2	11	93
KONDENGUI	12	93
BGRM	13	93
AHALA	14	93
NSIMALEN	15	93
MBALMAYO	16	93
NGOGI BAKOKO	17	93
KOUMASSI	18	93
BASSA	19	93
MAKEPE	20	93
DEIDO	21	93
DANGOTE	22	93
BONABERI	23	93
NJOMBE	24	93
OYOMABANG-1	25	225
MANGOMBE-1	26	225
LOGBABA-1	27	225
BEKOKO-1	28	225
OYOMABANG-2	29	93
EDEA	30	93
MANGOMBE-2	31	93
BAFOUSSAM	32	93
LOGBABA-3, 90 kV	78	93
OYOMABANG-3, 90 kV	79	93

A 3. Single line diagram of the SIG – disconnected mode (DM).

(a) Current SIG architecture

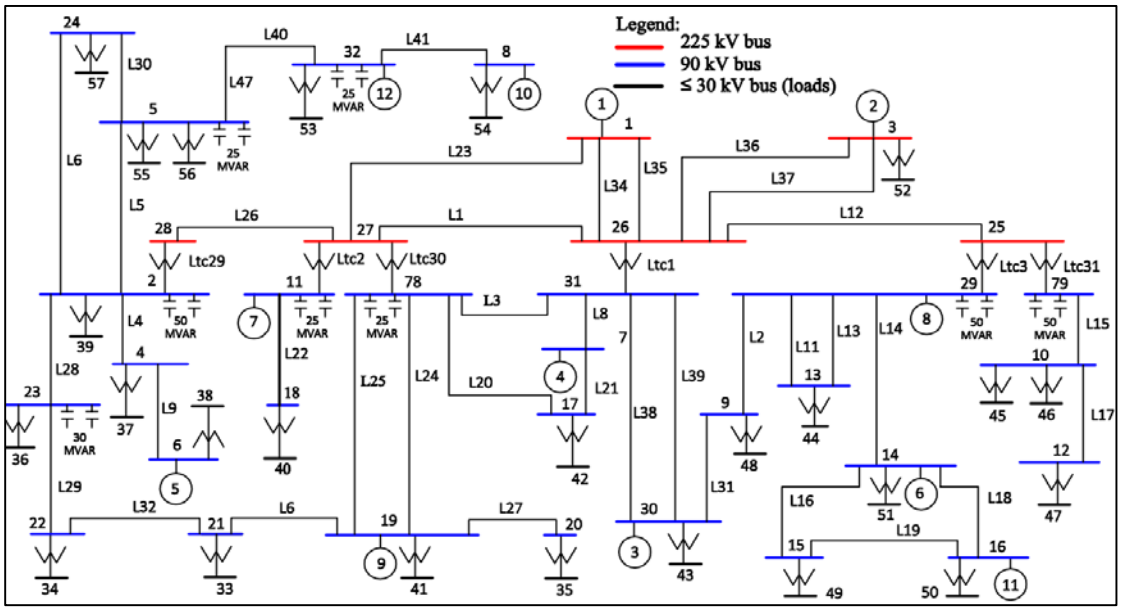

(b) Modified SIG architecture